Nebular and auroral emission lines of [Cl III] in the optical spectra of planetary nebulae

Francis P. Keenan*, Lawrence H. Aller†‡, Catherine A. Ramsbottom§, Kenneth L. Bell§, Fergal L. Crawford*, and Siek Hyung¶

*Department of Pure and Applied Physics, and §Department of Applied Mathematics and Theoretical Physics, The Queen's University of Belfast, Belfast BT7 1NN, Northern Ireland; †Astronomy Department, University of California, Los Angeles, CA 90095-1562; and ¶BohyunSan Observatory, P.O. Box 1, Jacheon Post Office, Young-Cheon, KyungPook, 770-820, South Korea

Contributed by Lawrence H. Aller, December 31, 1999

Electron impact excitation rates in Cl III, recently determined with the R-matrix code, are used to calculate electron temperature (T_e) and density (N_e) emission line ratios involving both the nebular (5517.7, 5537.9 Å) and auroral (8433.9, 8480.9, 8500.0 Å) transitions. A comparison of these results with observational data for a sample of planetary nebulae, obtained with the Hamilton Echelle Spectrograph on the 3-m Shane Telescope, reveals that the R_1 = I(5518 Å)/I(5538 Å) intensity ratio provides estimates of N_e in excellent agreement with the values derived from other line ratios in the echelle spectra. This agreement indicates that R_1 is a reliable density diagnostic for planetary nebulae, and it also provides observational support for the accuracy of the atomic data adopted in the line ratio calculations. However the [Cl III] 8433.9 Å line is found to be frequently blended with a weak telluric emission feature, although in those instances when the [Cl III] intensity may be reliably measured, it provides accurate determinations of T_e when ratioed against the sum of the 5518 and 5538 Å line fluxes. Similarly, the 8500.0 Å line, previously believed to be free of contamination by the Earth's atmosphere, is also shown to be generally blended with a weak telluric emission feature. The [Cl III] transition at 8480.9 Å is found to be blended with the He I 8480.7 Å line, except in planetary nebulae that show a relatively weak He I spectrum, where it also provides reliable estimates of T_e when ratioed against the nebular lines. Finally, the diagnostic potential of the near-UV [Cl III] lines at 3344 and 3354 Å is briefly discussed.

It was recognized in the 1940s that forbidden emission line ratios from nebular plasmas would provide a means for estimating electron densities (N_e) and temperatures (T_e) in the emitting layers. A difficulty has been to obtain N_e and T_e for the same ion, as different ions may be located in strata of differing parameters. For example, the intensity ratio of the auroral/nebular lines of [O III] have long been used to derive T_e for nebular plasmas, while the ratio of nebular lines of [O II] (3729 Å/3726 Å) and [S II] (6717 Å/6730 Å) have provided densities. Thus we obtain T_e in the O^{2+} zone and N_e in the O^+ or S^+ zone. To get N_e in the O^{2+} zone from [O III] lines we would need not only the usual optical region transitions, but also fine-structure infrared lines, which require observations from above the Earth's atmosphere.

The lines of [O II], [Ne IV], [S II], and [Ar IV] all arise from p^3 configurations and fall in the optical or near-UV part of the spectrum. By comparing the auroral or transauroral type transitions with those of nebular type (for example, the 4068 Å transauroral with the 6717, 6730 Å nebular transitions of [S II]), we can derive both T_e and N_e in the layers responsible for the emission. Accurate calculations for all relevant transitions have now been obtained for these ions (1–4).

Another ion of this group is Cl^{2+}, for which Ramsbottom *et al.* (5) have very recently calculated electron impact excitation rates by using the **R**-matrix method as adapted for the Opacity Project (6, 7). In this paper, we use the Ramsbottom *et al.* (5) results to derive emission line ratios applicable to planetary nebulae, and we compare these with high spectral resolution optical observations. Specifically, we assess the usefulness of [Cl III] line ratios as temperature and density diagnostics for planetary nebulae.

Atomic Data and Theoretical Line Ratios

The model ion for Cl III consisted of the three LS states within the $3s^23p^3$ ground configuration, namely ^4S, ^2D, and ^2P, making a total of five levels when the fine-structure splitting is included. Energies of all these levels were taken from Kelly (8). Test calculations including the higher-lying $3s3p^4$ terms were found to have a negligible effect on the $3s^23p^3$ level populations at the electron temperatures and densities typical of planetary nebulae, and hence these states were not included in the analysis.

Electron impact excitation rates for transitions in Cl III were obtained from Ramsbottom *et al.* (5), whereas for Einstein A-coefficients the calculations of Mendoza and Zeippen (9) were adopted. Our previous work on the isoelectronic ions S II (3) and Ar IV (4) has shown that excitation by protons is unimportant under nebular conditions, and hence this process has not been included in the present analysis.

Using the atomic data discussed above in conjunction with the statistical equilibrium code of Dufton (10), we derived relative Cl III level populations and hence emission line strengths for a range of electron temperatures (T_e = 5,000–20,000 K) and densities (N_e = $10^{1.5}$ to $10^{5.5}$ cm^{-3}). Details of the procedures involved and approximations made may be found in Dufton (10) and Dufton *et al.* (11). Given errors of typically ±10% in both the adopted electron excitation rates and A-values, we estimate that our derived theoretical line ratios should be accurate to ±15%.

The [Cl III] nebular emission line ratio

$$R_1 = I(3s^23p^3\ ^4S\text{–}3s^23p^3\ ^2D_{5/2})I(3s^23p^3\ ^4S - 3s^23p^3\ ^2D_{3/2})$$
$$= I(5517.7\ \text{Å})/I(5537.9\ \text{Å})$$

is a well known density diagnostic for planetary nebulae (12). However, Czyzak *et al.* (13) have pointed out that ratios in P-like ions involving both the nebular lines and the auroral $3s^23p^3\ ^2D\text{–}3s^23p^3\ ^2P$ transitions should allow both T_e and N_e to be derived, and illustrated this by plotting theoretical results for [S II]. In Figs. 1 and 2 we therefore plot R_1 against the auroral/nebular line ratios

$$R_2 = I(3s^23p^3\ ^2D_{3/2}\text{–}3s^23p^3\ ^2P_{3/2}/I(3s^23p^3\ ^4S\text{–}3s^23p^3\ ^2D_{3/2,5/2})$$
$$= I(8433.9\ \text{Å})/I(5517.7 + 5537.9\ \text{Å})$$

Abbreviation: HES, Hamilton Echelle Spectrograph.

‡To whom reprint requests should be addressed. E-mail: aller@astro.ucla.edu.

The publication costs of this article were defrayed in part by page charge payment. This article must therefore be hereby marked "*advertisement*" in accordance with 18 U.S.C. §1734 solely to indicate this fact.

Article published online before print: *Proc. Natl. Acad. Sci. USA*, 10.1073/pnas.070590597. Article and publication date are at www.pnas.org/cgi/doi/10.1073/pnas.070590597

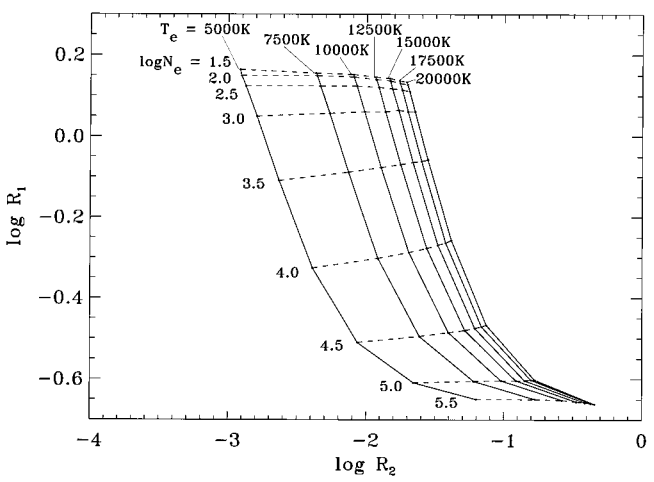

Fig. 1. Plot of the theoretical [Cl III] nebular emission line ratio $R_1 = I(3s^2 3p^3\ ^4S–3s^2 3p^3\ ^2D_{5/2})/I(3s^2 3p^3\ ^4S–3s^2 3p^3\ ^2D_{3/2}) = I(5518\ Å)/I(5538\ Å)$ against the auroral/nebular ratio $R_2 = I(3s^2 3p^3\ ^2D_{3/2}–3s^2 3p^3\ ^2P_{3/2})/I(3s^2 3p^3\ ^4S–3s^2 3p^3\ ^2D_{3/2,5/2}) = I(8434\ Å)/I(5518 + 5538\ Å)$, where I is in energy units, for a range of electron temperatures (T_e = 5,000–20,000 K in steps of 2,500 K) and logarithmic electron densities (log N_e = 1.5–5.5 in steps of 0.5 dex; N_e in cm^{-3}). Points of constant T_e are connected by solid lines, whereas those of constant N_e are joined by dashed lines.

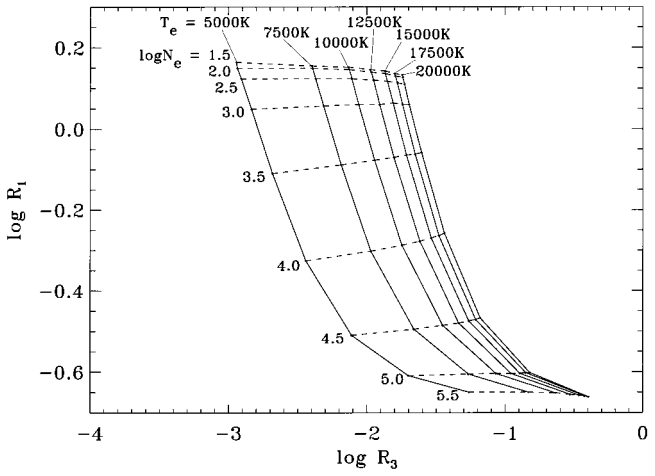

Fig. 2. Same as Fig. 1, except for R_1 against $R_3 = I(3s^2 3p^3\ ^2D_{3/2}–3s^2 3p^3\ ^2P_{1/2})/I(3s^2 3p^3\ ^4S–3s^2 3p^3\ ^2D_{3/2,5/2}) = I(8500\ Å)/I(5518 + 5538\ Å)$.

and

$$R_3 = I(3s^2 3p^3\ ^2D_{3/2}–3s^2 3p^3\ ^2P_{1/2}/I(3s^2 3p^3\ ^4S–3s^2 3p^3\ ^2D_{3/2,5/2}) = I(8500.0\ Å)/I(5517.7 + 5537.9\ Å),$$

respectively, for a grid of (T_e, log N_e) values. Clearly, measurements of R_1 and R_2, or R_1 and R_3, should in principle allow the simultaneous determination of T_e and N_e for the [Cl III] emitting region of the nebula. We note that the theoretical ratios

$$R_4 = I(3s^2 3p^3\ ^2D_{3/2}–3s^2 3p^3\ ^2P_{3/2})/I(3s^2 3p^3\ ^4S–3s^2 3p^3\ ^2D_{3/2,5/2}) = I(8480.9\ Å)/I(5517.7 + 5537.9\ Å)$$

and

$$R_5 = I(3s^2 3p^3\ ^2D_{5/2}–3s^2 3p^3\ ^2P_{1/2})I(3s^2 3p^3\ ^4S–3s^2 p^3\ ^2D_{3/2,5/2}) = I(8548.0\ Å)/I(5517.7 + 5537.9\ Å)$$

have the same temperature and density dependence as R_2 and R_3, respectively, because of common upper levels, but with

$$R_4 = 0.973 \times R_2$$

and

$$R_5 = 0.328 \times R_3.$$

Observational Data

Observational data were obtained with the Hamilton Echelle Spectrograph (HES) at the coudé focus of the 3-m Shane Telescope at the Lick Observatory during several observing runs between 1987 and 1994. The echelle grating, which is ruled with 316 grooves per cm to achieve the best possible match with an 800 × 800 TI charge-coupled device detector, permits coverage of the wavelength range 3,600–10,300 Å. Each order contains only a small portion of spectrum, and these are separated with the aid of a pair of low-dispersion prisms, which serve as cross dispersers. The data we have used here were secured in the context of a spectral survey of several planetaries of high surface brightness. For nebular observations, a slit width of 640 μm (1.16 arcsec) and a slit length of 4 arcsec were adopted, giving a spectral resolution of ~0.2 Å (full width at half maximum). These choices were imposed by constraints on spectral purity (for slit width) and overlapping orders, especially in the red (for slit length). The total area accepted by the slit is generally much smaller than the whole nebular image. In addition to the usual exposures on laboratory arcs and appropriate comparison stars, one also needs a diffuse continuous source to allow for pixel-to-pixel sensitivity variations. Our basic observing and reduction procedures are described in Keyes *et al.* (14) and Hyung (15).

In Table 1 we list the planetary nebulae considered in the present analysis, their date of observation, and the measured intensities (I) of the [Cl III] 5518, 5538, 8434, 8481, and 8500 Å lines [on the scale $I(H\beta) = 100$]. The $3s^2 3p^3\ D_{5/2}–3s^2 3p^3\ ^2P_{1/2}$ line, predicted to lie at a wavelength of 8548.0 Å (16), is too weak to be detected in our data. However we note that Péquignot and Baluteau (17) have very marginally identified the line in the wing of the strong H I 8545.4 Å feature, in the spectrum of NGC 7027.

The [Cl III] line intensities in Table 1 have been corrected for interstellar extinction, using the extinction curve of Seaton (18) in conjunction with the interstellar extinction coefficient $C = 1.47E(B - V) = \log[I^i(H\beta)/I^o(H\beta)]$, where $I^i(H\beta)$ and $I^o(H\beta)$ are the intrinsic and observed Hβ line intensities, respectively. Values of C, listed in Table 1, have been taken from the references given as footnotes to Table 3, or derived from a comparison of observed hydrogen recombination line flux ratios with calculations (19).

The resultant values of R_1, R_2, R_3, and R_4 are given in Table 2. We estimate that the uncertainties in the line intensities should be approximately ±10% for $I \geq 1.0$, ±15% for $0.5 \leq I < 1.0$, and ±20% for $I < 0.5$. Hence the line ratios should be accurate to typically ±20–25%. To illustrate the quality of the observational data, in Figs. 3, 4, and 5 we plot the HES spectrum of NGC 6572 in the 5514–5545 Å, 8420–8475 Å, and 8450–8505 Å wavelength regions, respectively.

Results and Discussion

In Table 3 we summarize the electron temperatures and logarithmic electron densities derived from the observed (R_1, R_2), (R_1, R_3), and (R_1, R_4) line pairs in conjunction with Figs. 1 and 2. As is clear from these figures, R_1 is sensitive primarily to changes in N_e, whereas the other ratios depend strongly on both temperature and density. Hence in those instances where the observed R_2, R_3, or R_4 ratios lie outside the range of values given

Table 1. Summary of [Cl III] observations

Object	Observation date	I(5518 Å)	I(5538 Å)	I(8434 Å)	I(8481 Å)	I(8500 Å)	C*
NGC 2440	Nov. 18, 1989	5.40−1	6.21−1	—	—	9.00−2	0.53
NGC 6537	June 15, 1992	3.85−1	9.16−1	1.91−2	—	—	1.80
NGC 6572	Aug. 5, 1990	1.58−1	3.75−1	1.50−2	1.70−2	2.10−2	0.40
NGC 6572	Sept. 1, 1991	1.70−1	3.97−1	2.10−2	2.40−2	3.10−2	0.40
NGC 6741	Sept. 30, 1991	6.32−1	1.02+0	3.80−2	6.40−2	—	1.10
NGC 6884	Aug. 30, 1994	2.73−1	4.99−1	4.50−2	—	—	1.10
NGC 7009	July 27, 1988	2.97−1	4.08−1	2.90−2	2.50−2	—	0.08
NGC 7027	Sept. 4, 1987	1.67−1	6.37−1	8.60−2	7.10−2	8.60−2	1.37
NGC 7662	Aug. 28, 1988	2.70−1	3.35−1	—	5.70−2	—	0.10
IC 2165	Nov. 17, 1989	3.30−1	3.70−1	—	3.00−2	4.00−2	0.68
IC 4997	Aug. 3, 1990	4.60−2	1.20−1	1.50−2	2.00−2	1.70−2	0.80
IC 4997	Aug. 30, 1991	6.10−2	1.31−1	1.30−2	3.30−2	2.80−2	0.80
Hubble 12	Aug. 6, 1990	5.00−2	1.35−1	6.00−2	6.20−2	6.40−2	1.35

Line intensities I (in energy units), corrected for interstellar extinction, are given relative to $I(\mathrm{H}\beta) = 100$. $A \pm B$ implies $A \times 10^{\pm B}$.

*Interstellar extinction coefficient $C = 1.47\mathrm{E}(B-V) = \log[I^{i}(\mathrm{H}\beta)/I^{o}(\mathrm{H}\beta)]$, where $I^{i}(\mathrm{H}\beta)$ and $I^{o}(\mathrm{H}\beta)$ are the intrinsic and observed Hβ line intensities, respectively.

in Figs. 1 and 2 (so that the simultaneous determination of T_e and $\log N_e$ is not possible), we have still been able to measure $\log N_e$ from R_1, by adopting $T_e = 10{,}000$ K. We note that varying the adopted temperature from 5,000 K to 20,000 K (i.e., the full range in Fig. 1 or 2) will change the value of $\log N_e$ derived from R_1 only by at most ± 0.1 dex.

Also listed in Table 3 are the plasma parameters, denoted $(T_e, \log N_e)_{\mathrm{other}}$, determined from other line ratios in the planetary nebulae that have similar ionization potentials and hence similar spatial distributions to [Cl III], such as $I(3729\ \text{Å})/I(3726\ \text{Å})$ and $I(7320\ \text{Å})/I(3726 + 3729\ \text{Å})$ in [O II]. These T_e and N_e estimates have been deduced from diagnostic diagrams constructed with the same HES data as those used for the [Cl III] observations. Hence the values of $(T_e, \log N_e)_{\mathrm{other}}$ should apply to the region of the planetary nebula for which the [Cl III] observations were obtained, so that the [Cl III] results should be directly comparable to these. Plasma parameters from the literature, on the other hand, often refer to the whole nebular image. The sources of the diagnostic diagrams used to derive $(T_e, \log N_e)_{\mathrm{other}}$ are listed in the last column of Table 3.

For all of the planetary nebulae in Table 3, the derived electron densities are in very good agreement with those deduced from other line ratios in the HES observations, with discrepancies that average only 0.1 dex. This agreement indicates that R_1 is a reliable density diagnostic for planetary nebulae, and also provides support for the accuracy of the atomic physics data adopted in the calculations of the ratio.

However, values of T_e could be measured for only a number of objects in Table 3, with (as noted above) the temperature being indeterminate in several instances because the observed R_2, R_3, or R_4 ratio lies outside the range of theoretical values given in Fig. 1 or 2. These discrepancies are most probably due to blending of the observational data. In the case of the 8433.9 Å line in the R_2 ratio, we note that this transition is sometimes blended with a weak telluric emission feature (20). However, reliable estimates of the 8434 Å line intensity can be made if the effect of the telluric feature is minimized by, for example, observing at low air mass and away from twilight. From Table 3, we see that reliable measurements of R_1 are available for a few planetary nebulae, which give temperatures in good agreement with those determined from other diagnostics, with discrepancies that average only 1,200 K.

The 8480.9 Å line in the R_4 ratio is blended with the 8480.7 Å transition of He I (21). As a result, the [Cl III] line can be reliably measured only when the He I spectrum is relatively weak, which is the case for NGC 6572 and NGC 7027. For these

Table 2. [Cl III] emission line ratios

Object	R_1 $\frac{I(5518\ \text{Å})}{I(5538\ \text{Å})}$	R_2 $\frac{I(8434\ \text{Å})}{I(5518 + 5538\ \text{Å})}$	R_3 $\frac{I(8500\ \text{Å})}{I(5518 + 5538\ \text{Å})}$	R_4 $\frac{I(8481\ \text{Å})}{I(5518 + 5538\ \text{Å})}$
NGC 2440	8.70−1	—	7.75−2	—
NGC 6537	4.20−1	1.47−2	—	—
NGC 6572*	4.21−1	2.81−2	3.94−2	3.19−2
NGC 6572†	4.28−1	3.70−2	5.47−2	4.23−2
NGC 6741	6.20−1	2.30−2	—	3.87−2
NGC 6884	5.47−1	5.83−2	—	—
NGC 7009	7.28−1	4.11−2	—	3.55−2
NGC 7027	2.62−1	1.07−1	1.07−1	8.83−2
NGC 7662	8.06−1	—	—	9.42−2
IC 2165	8.92−1	—	5.71−2	4.29−2
IC 4997*	3.83−1	9.04−2	1.02−1	1.20−1
IC 4997†	4.66−1	6.77−2	1.46−1	1.72−1
Hubble 12	3.70−1	3.24−1	3.46−1	3.35−1

$A-B$ implies $A \times 10^{-B}$.

*Observations taken in 1990.

†Observations taken in 1991.

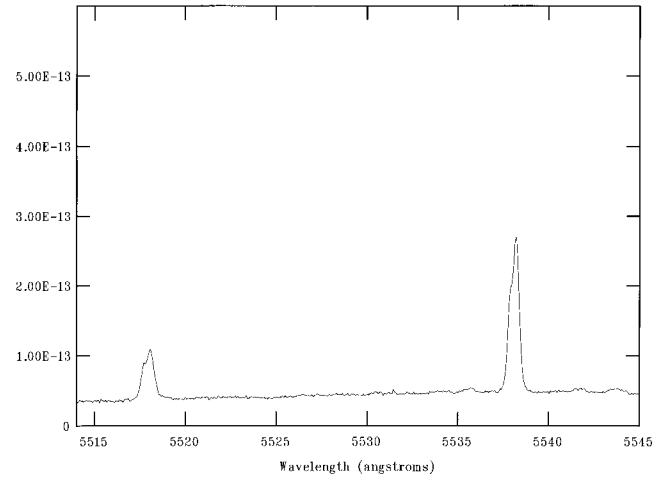

Fig. 3. Plot of the Hamilton echelle spectrum of the planetary nebula NGC 6572, obtained on Sept. 1, 1991, in the wavelength interval 5514–5545 Å, showing the [Cl III] 5517.7 and 5537.9 Å lines, where the flux is in units of erg·cm^{-2}·sec^{-1}·Å^{-1}. We note that the structure in the [Cl III] emission lines is due to shell expansion within the nebula. Radial velocity and interstellar extinction corrections (C = 0.4) have not been applied to this spectral scan.

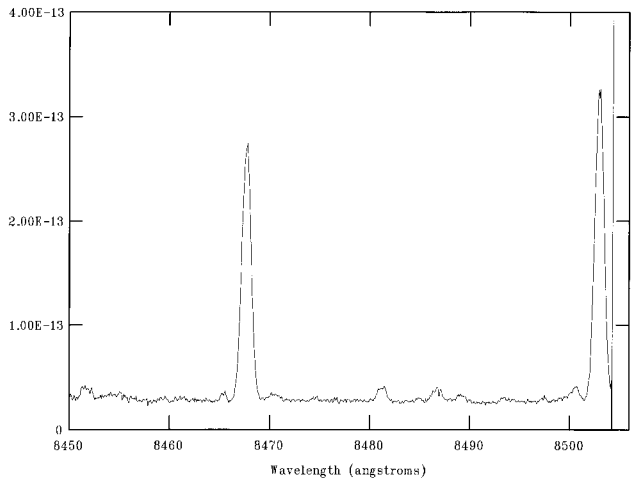

Fig. 5. Plot of the Hamilton echelle spectrum of the planetary nebula NGC 6572, obtained on Sept. 1, 1991, in the wavelength interval 8450–8505 Å, showing the [Cl III] 8480.9 and 8500.0 Å lines, where the flux is in units of erg·cm^{-2}·sec^{-1}·Å^{-1}. Also shown are the 8467.3 and 8502.5 Å emission lines of H I. We note that the structure in the emission lines is due to shell expansion within the nebula. Radial velocity and interstellar extinction corrections (C = 0.4) have not been applied to this spectral scan.

objects, the temperatures indicated by the R_4 ratios are similar to those determined from other diagnostics.

Most of the observed values of R_3, which contains the 8500.0 Å line, are much larger than those predicted from Fig. 2. For example, the plasma parameters $(T_e, \log N_e)_{other}$ = (12,500, 4.4) for Hubble 12 in Table 3 imply a theoretical R_3 = 0.040 from Fig. 2, yet the observed ratio is R_3 = 0.346. Blending would appear to be the obvious reason for this discrepancy, but the [Cl III] 8500.0 Å line is always well resolved from the nearby H I 8502.5 Å feature in the HES spectra, as shown in Fig. 5. However, there is a very weak telluric emission line at 8500.0 Å (20), which is probably the source of the blend. Support for this explanation is provided by the fact that the R_3 ratios in Table 3 for NGC 6572 and NGC 7027 give T_e estimates in good agreement with those determined from other diagnostics, indicating that the [Cl III] 8500 Å line intensity must be reliably measured in these objects. As noted previously, the 8434 Å line in NGC 6572 and NGC 7027 is uncontaminated by telluric blending, implying that the 8500 Å transition should be similarly unaffected, which is observed to be the case. The 8500 Å line was previously believed to be uncontaminated by the Earth's atmosphere (22). However measurements of this feature must be treated with caution in the future and, as with the 8434 Å transition, should be used as a diagnostic only if free from telluric blending. This will be the case for space-based observations from, for example, the Space Telescope Imaging Spectrograph, and the [Cl III] lines in such data may therefore be used with confidence to determine plasma parameters.

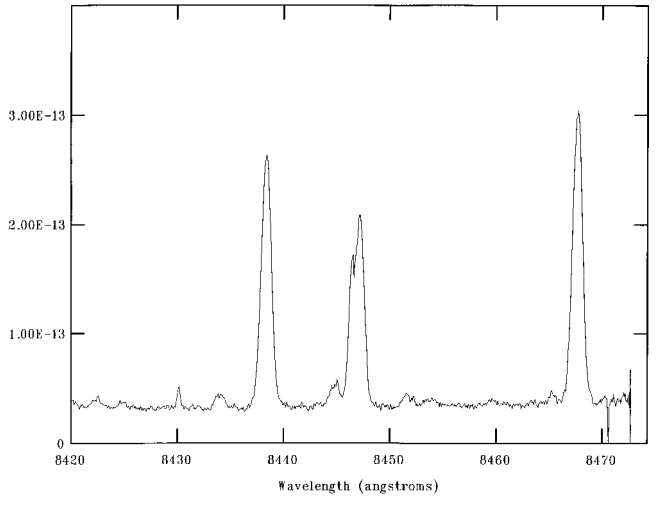

Fig. 4. Plot of the Hamilton echelle spectrum of the planetary nebula NGC 6572, obtained on Sept. 1, 1991, in the wavelength interval 8420–8475 Å, showing the [Cl III] 8433.9 Å line, where the flux is in units of erg·cm^{-2}·sec^{-1}·Å^{-1}. Also shown are emission lines due to H I at 8438.0 Å, Si I at 8444.5 Å, O I at 8446.5 Å, S I at 8451.6 Å, and H I at 8467.3 Å. We note that the structure in the emission lines is due to shell expansion within the nebula. Radial velocity and interstellar extinction corrections (C = 0.4) have not been applied to this spectral scan.

Finally, we note that the [Cl III] emission line ratios

$$R_6 = I(3s^2 3p^3\ ^4\mathrm{S}–3s^2 3p^3\ ^2\mathrm{P}_{3/2})/I(3s^2 3p^3\ ^4\mathrm{S}–3s^2 3p^3\ ^2\mathrm{D}_{3/2,5/2})$$
$$= I(3343.7\ \text{Å})/I(5517.7 + 5537.9\ \text{Å})$$

and

$$R_7 = I(3s^2 3p^3\ ^4\mathrm{S}–3s^2 3p^3\ ^2\mathrm{P}_{1/2})/I(3s^2 3p^3\ ^4\mathrm{S}–3s^2 3p^3\ ^2\mathrm{D}_{3/2,5/2})$$
$$= I(3354.4\ \text{Å})/I(5517.7 + 5537.9\ \text{Å})$$

have the same temperature and density dependence as R_2 and R_3, respectively, because of common upper levels, but with

$$R_6 = 5.88 \times R_2$$

and

$$R_7 = 2.55 \times R_3.$$

Hence the observed (R_1, R_6) or (R_1, R_7) line pairs could be used in conjunction with Figs. 1 and 2 to determine T_e and $\log N_e$, as noted by Czyzak *et al.* (13). Unfortunately, the 3344 and 3354 Å lines of [Cl III] lie in a relatively unexplored region of the nebular spectrum, at least at high spectral resolution, because of the difficulty of observing in the near-UV. However, with the

Table 3. Derived [Cl III] electron temperatures and densities

Object	(T_e, log N_e) (R_1, R_2)	(R_1, R_3)	(R_1, R_4)	(T_e, log N_e)$_{other}$	Ref.*
NGC 2440	—	*I*, 3.4	—	11,750, 3.7	22
NGC 6537	7,500, 4.2	—	—	9,200, 4.3	24
NGC 6572†	10,000, 4.2	14,000, 4.3	11,000, 4.2	11,000, 4.2	25
NGC 6572‡	12,500, 4.2	*I*, 4.2	14,000, 4.2	11,000, 4.2	25
NGC 6741	12,000, 3.8	—	*I*, 3.8	11,750, 3.7	26
NGC 6884	*I* 3.9	—	—	11,750, 4.1	21
NGC 7009	*I*, 3.6	—	*I*, 3.6	11,500, 3.6	27
NGC 7027	12,500, 4.9	13,500, 4.9	11,000, 4.9	14,000, 4.8	14
NGC 7662	—	—	*I*, 3.5	12,000, 3.7	28
IC 2165	—	*I*, 3.4	*I*, 3.4	9,750, 3.6	15
IC 4997†	*I*, 4.3	*I*, 4.3	*I*, 4.3	10,000, 4.2	29
IC 4997‡	*I*, 4.1	*I*, 4.1	*I*, 4.1	10,000, 4.2	29
Hubble 12	*I*, 4.3	*I*, 4.3	*I*, 4.3	12,500, 4.4	30

T_e values are in K, N_e values are in cm^{-3}. *I* indicates that T_e was indeterminate due to the observed R_2, R_3, or R_4 line ratio lying outside the range of values given in Fig. 1 or 2. In these instances, log N_e was deduced from R_1 by adopting T_e = 10,000 K.
*References for sources of (T_e, log N_e)$_{other}$.
†Observations taken in 1990.
‡Observations taken in 1991.

increasing blue sensitivity being achieved by charge-coupled devices, it is hoped that high-resolution spectra of these lines will be routinely available in the future. The near-UV features will not have the problem with telluric blends experienced by the longer-wavelength transitions, and hence should provide reliable temperature and density estimates. We stress, however, that they must be observed at high spectral resolution as, for example, the [Cl III] 3344 Å line is blended with [Ne V] 3345 Å at low dispersion (23).

C.A.R. is grateful to the Particle Physics and Astronomy Research Council for financial support; F.L.C. holds a research studentship from the Department of Education for Northern Ireland. This research was supported by National Science Foundation Grants AST 90–14133, AST 93–13991, and AST 94–16985, and Space Telescope Science Institute Grant AR-06372.01–95A, to the University of California, Los Angeles. We also gratefully acknowledge the support provided by North Atlantic Treaty Organization travel grant CRG.930722, and Star 98–2-500–00 to the Korea Astronomy Observatory/BohyunSan Optical Astronomy Observatory sponsored by the Korean Ministry of Science and Technology.

1. Keenan, F. P., Aller, L. H., Bell, K. L., Crawford, F. L., Feibelman, W. A., Hyung, S., McKenna, F. C. & McLaughlin, B. M. (1999) *Mon. Not. R. Astron. Soc.* **304,** 27–34.
2. Keenan, F. P., Aller, L. H., Bell, K. L., Espey, B., Feibelman, W. A., Hyung, S., McKenna, F. C. & Ramsbottom, C. A. (1998) *Mon. Not. R. Astron. Soc.* **295,** 683–690.
3. Keenan, F. P., Aller, L. H., Bell, K. L., Hyung, S., McKenna, F. C. & Ramsbottom, C. A. (1996) *Mon. Not. R. Astron. Soc.* **281,** 1073–1080.
4. Keenan, F. P., McKenna, F. C., Bell, K. L., Ramsbottom, C. A., Wickstead, A. W., Aller, L. H. & Hyung, S. (1997) *Astrophys. J.* **487,** 457–462.
5. Ramsbottom, C. A., Bell, K. L. & Keenan, F. P. (1999) *Mon. Not. R. Astron. Soc.* **307,** 669–676.
6. Seaton, M. J. (1987) *J. Phys. B* **20,** 6363–6378.
7. Berrington, K. A., Burke, P. G., Butler, K., Seaton, M. J., Storey, P. J., Taylor, K. T. & Yu, Y. (1987) *J. Phys. B* **20,** 6379–6397.
8. Kelly, R. L. (1987) *J. Phys. Chem. Ref. Data* **16,** 1371–1678.
9. Mendoza, C. & Zeippen, C. J. (1982) *Mon. Not. R. Astron. Soc.* **198,** 127–139.
10. Dufton, P. L. (1977) *Comput. Phys. Commun.* **13,** 25–38.
11. Dufton, P. L., Berrington, K. A., Burke, P. G. & Kingston, A. E. (1978) *Astron. Astrophys.* **62,** 111–120.
12. Stanghellini, L. & Kaler, J. B. (1989) *Astrophys. J.* **343,** 811–827.
13. Czyzak, S. J., Keyes, C. D. & Aller, L. H. (1986) *Astrophys. J. Suppl.* **61,** 159–175.
14. Keyes, C. D., Aller, L. H. & Feibelman, W. A. (1990) *Publ. Astron. Soc. Pacific* **102,** 59–76.
15. Hyung, S. (1994) *Astrophys. J. Suppl.* **90,** 119–148.
16. Kaufman, V. & Sugar, J. (1986) *J. Phys. Chem. Ref. Data* **15,** 321–426.
17. Péquignot, D. & Baluteau, J.-P. (1988) *Astron. Astrophys.* **206,** 298–315.
18. Seaton, M. J. (1979) *Mon. Not. R. Astron. Soc.* **187,** 73P–76P.
19. Hummer, D. G. & Storey, P. J. (1987) *Mon. Not. R. Astron. Soc.* **224,** 801–820.
20. Osterbrock, D. E., Fulbright, J. P., Martel, A. R., Keane, M. J., Trager, S. C. & Basri, G. (1996) *Publ. Astron. Soc. Pacific* **108,** 277–308.
21. Hyung, S., Aller, L. H. & Feibelman, W. A. (1997) *Astrophys. J. Suppl.* **108,** 503–513.
22. Hyung, S. & Aller, L. H. (1998) *Publ. Astron. Soc. Pacific* **110,** 466–479.
23. Aller, L. H. & Czyzak, S. J. (1983) *Astrophys. J. Suppl.* **51,** 211–248.
24. Aller, L. H., Hyung, S. & Feibelman, W. A. (1999) *Proc. Nat. Acad. Sci. USA* **96,** 5366–5371.
25. Hyung, S., Aller, L. H. & Feibelman, W. A. (1994) *Mon. Not. R. Astron. Soc.* **269,** 975–997.
26. Hyung, S. & Aller, L. H. (1997) *Mon. Not. R. Astron. Soc.* **292,** 71–85.
27. Hyung, S. & Aller, L. H. (1995) *Mon. Not. R. Astron. Soc.* **273,** 973–991.
28. Hyung, S. & Aller, L. H. (1997) *Astrophys. J.* **491,** 242–253.
29. Hyung, S., Aller, L. H. & Feibelman, W. A. (1994) *Astrophys. J. Suppl.* **93,** 465–483.
30. Hyung, S. & Aller, L. H. (1996) *Mon. Not. R. Astron. Soc.* **278,** 551–564.